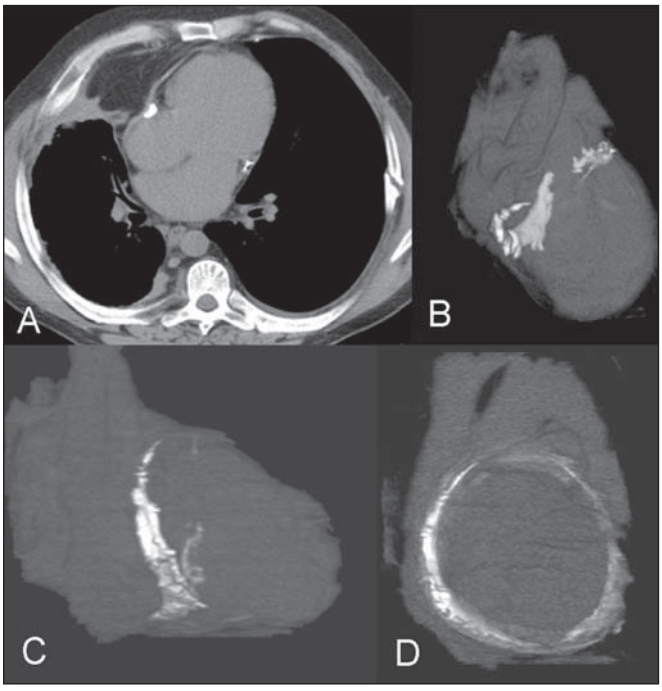

Figure 1. Axial computed tomography image (**A**) and volume-rendered reconstructions (**B–D**) showing a calcified pericardial band encircling the left ventricular cavity at the level of the atrioventricular groove.

Constrictive pericarditis is characterized by thick pericardial fibrosis and frequent calcification that progressively impairs diastolic filling of the heart, with associated symptoms of heart failure[1]. Annular constrictive pericarditis is extremely rare, and few similar cases have been reported[1]. Previous pericardiectomy, congenital heart disease, and complications of tuberculosis may be the leading causes of this condition. Depending on the location of the pericardial constriction, the clinical presentation of localized constriction may differ, including obstruction of the right ventricular outflow tract, coronary obstruction, and pulmonary stenosis[1–3]. The imaging evaluation of cardiovascular calcifications has been the subject of a series of recent publications in the Brazilian radiology literature[4–7]. Multislice computed tomography may be an important tool for the precise identification of annular constrictive pericarditis[8].

REFERENCES

1. Butany J, El Demellawy D, Collins MJ, et al. Constrictive pericarditis: case presentation and review of the literature. Can J Cardiol. 2004;20: 1137–44.
2. Nigri A, Mangieri E, Martuscelli E, et al. Pulmonary trunk stenosis due to constriction by a pericardial band. Am Heart J. 1987;114:448–50.
3. Mounsey P. Annular constrictive pericarditis. With an account of a patient with functional pulmonary, mitral, and aortic stenosis. Br Heart J. 1959;21:325–34.
4. Barbosa JHO, Santos AC, Salmon CEG. Susceptibility weighted imaging: differentiating between calcification and hemosiderin. Radiol Bras. 2015;48:93–100.
5. Neves PO, Andrade J, Monção H. Coronary anomalies: what the radiologist should know. Radiol Bras. 2015;48:233–41.
6. Araújo Neto CA, Oliveira Andrade AC, Badaró R. Intima-media complex in the investigation of atherosclerosis in HIV-infected patients [Letter to the Editor]. Radiol Bras. 2014;47(1):x.
7. Brasileiro Junior VL, Luna AHB, Sales MAO, et al. Reliability of digital panoramic radiography in the diagnosis of carotid artery calcifications. Radiol Bras. 2014;47:28–32.
8. Matsuno Y, Shimabukuro K, Ishida N, et al. Off-pump complete pericardiectomy for an unusual case of annular constrictive pericarditis. Ann Thorac Surg. 2012;94:e45–7.

Bruno Hochhegger[1], Klaus L. Irion[2], Gláucia Zanetti[3], Edson Marchiori[3]

1. Universidade Federal de Ciências da Saúde de Porto Alegre (UFCSPA), Porto Alegre, RS, Brazil. 2. Liverpool Heart and Chest Hospital – NHS Trust, Liverpool, United Kingdom. 3. Universidade Federal do Rio de Janeiro (UFRJ), Rio de Janeiro, RJ, Brazil. Mailing address: Dr. Edson Marchiori. Rua Thomaz Cameron, 438, Valparaíso. Petrópolis, RJ, Brazil, 25685-120. E-mail: edmarchiori@gmail.com.

http://dx.doi.org/10.1590/0100-3984.2015.0151

Post-Oberlin procedure cortical neuroplasticity in traumatic injury of the upper brachial plexus

Dear Editor,

A 27-year-old left-handed male injured his left arm in a motorcycle accident. The clinical examination showed a lack of movement in the left forearm and shoulder, with normal movement of the left hand. Magnetic resonance imaging (MRI) showed avulsion of left upper nerve roots (C5 and C6) of the brachial plexus, caused by traumatic lesion. He underwent neurotization by the Oberlin procedure and transfer of the accessory nerve to the suprascapular nerve three months after the accident[1]. The first signs of re-innervation of the biceps muscle appeared two months after the surgical procedure. The patient later showed significant signs of recovery.

We selected this patient to undergo functional MRI (fMRI). For the fMRI acquisition, we also selected one healthy control volunteer who was matched to the patient for age, gender, and handedness. Both subjects underwent MRI in order to compose a structural sequence with anatomical images. In the functional sequence, we employed the following acquisition parameters: repetition time = 2000 ms; echo time = 30 ms; flip angle = 90°; matrix = 64 × 64; field of view = 240 mm; voxel resolution = 3.75 × 3.75 × 5 mm; slice thickness = 5 mm; sagittal plane, 22 planes.

The motor tasks consisted of elbow flexion and hand grasping, in a "block" design: hand grasping of the dominant injured limb (left upper limb) and elbow flexion of the injured and healthy limbs. All motor tasks were alternated with a rest period (there were 100 dynamics per block, and there were 10 rest dynamics for each set of 10 task dynamics). Ten blocks of each state (resting and limb movement) were used. The patient and the healthy volunteer performed the same tasks. The MRI of the patient showed no anatomical alterations. After family-wise error correction at a value of $p < 0.05$, all fMRI scans acquired during the motor tasks showed main activation of the contralateral hemisphere in the areas that correspond to the primary motor cortex (Figure 1), as follows: forearm and hand for hand grasping of the left upper limb; arm, forearm, hand, and face for left elbow flexion; arm and forearm for flexion of the right upper limb. The MRI of the healthy volunteer also showed no anatomical alterations.

In the case reported here, fMRI was effective in identifying the cortical activations. The comparison between the patient and the healthy volunteer showed that the areas of cortical activation were quite similar, as were the activation peaks. The detectable reactivation of the cortical area in the patient during flexion of the injured elbow corresponded to the arm area in the motor homunculus of the volunteer[2–8]. The cortical activations in this case were similar to those reported in previous studies that applied

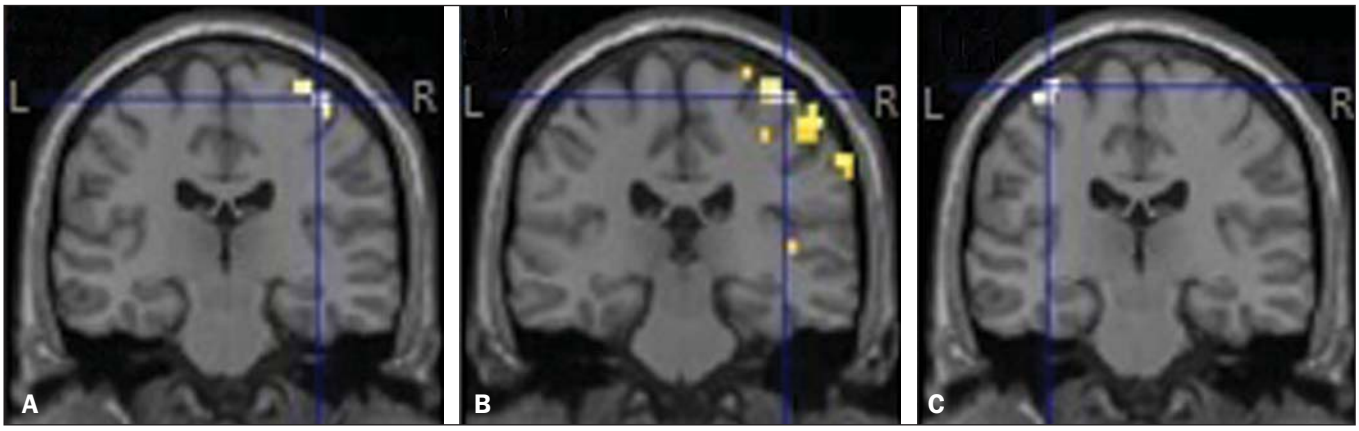

Figure 1. Cortical activation during motor tasks in the patient. Only the cortex is represented, and the peak of activation in the coordinates were as follows: **A:** left hand, x = 38 mm, y = –22 mm, z = 65 mm; **B:** left elbow, x = 42 mm, y = –26 mm, z = 65 mm; **C:** right elbow, x = –33 mm, y = –18 mm, z = 70 mm. (R, right hemisphere; L, left hemisphere).

extraplexus nerve transfer techniques, the areas of activation mainly being located in the contralateral cortex[2–8].

This study has some limitations. We presented the patient data only in comparison with those of a single control participant, rather than with a group of control, and both data sets were acquired at only one time point. In addition, the patient did not undergo a pre-operative fMRI scan.

REFERENCES

1. Oberlin C, Béal D, Leechavengvongs S, et al. Nerve transfer to biceps muscle using a part of ulnar nerve for C5-C6 avulsion of the brachial plexus: anatomical study and report of four cases. J Hand Surg Am. 1994;19:232–7.
2. Malessy MJ, van der Kamp W, Thomeer RT, et al. Cortical excitability of the biceps muscle after intercostal-to-musculocutaneous nerve transfer. Neurosurgery. 1998;42:787–95.
3. Iwase Y, Mashiko T, Ochiai N, et al. Postoperative changes on functional mapping of the motor cortex in patients with brachial plexus injury: comparative study of magnetoencephalography and functional magnetic resonance imaging. J Orthop Sci. 2001;6:397–402.
4. Malessy MJ, Bakker D, Dekker AJ, et al. Functional magnetic resonance imaging and control over the biceps muscle after intercostal-musculocutaneous nerve transfer. J Neurosurg. 2003;98:261–8.
5. Beaulieu JY, Blustajn J, Teboul F, et al. Cerebral plasticity in crossed C7 grafts of the brachial plexus: an fMRI study. Microsurgery. 2006; 26:303–10.
6. Sokki AM, Bhat DI, Devi BI. Cortical reorganization following neurotization: a diffusion tensor imaging and functional magnetic resonance imaging study. Neurosurgery. 2012;70:1305–11.
7. Hua XY, Liu B, Qiu YQ, et al. Long-term ongoing cortical remodeling after contralateral C-7 nerve transfer. J Neurosurg. 2013;118:725–9.
8. Dimou S, Biggs M, Tonkin M, et al. Motor cortex neuroplasticity following brachial plexus transfer. Front Hum Neurosci. 2013;7:500.

Ana Caroline Siquara de Sousa[1], José Fernando Guedes-Corrêa[1]

1. Hospital Universitário Gaffrée e Guinle – Universidade Federal do Estado do Rio de Janeiro (Unirio), Rio de Janeiro, RJ, Brazil. Mailing address: Dr. José Fernando Guedes-Corrêa. Hospital Universitário Gaffrée e Guinle – Departamento de Neurocirurgia. Rua Mariz e Barros, 775, Tijuca. Rio de Janeiro, RJ, Brazil, 20270-004. E-mail: neuroguedes@yahoo.com.br.

http://dx.doi.org/10.1590/0100-3984.2015.0082

Hughes-Stovin syndrome: an unusual cause of pulmonary artery aneurysms

Dear Editor,

A 43-year-old male presented with a two-month history of persistent cough and fever, associated with recurrent episodes of superficial thrombophlebitis and venous thrombosis of the lower limbs. Physical examination revealed no evidence of oral or genital ulcers. Ancillary tests showed negative blood culture; no thrombophilia or neoplasia; negative serology; mild normocytic, normochromic anemia; elevated C-reactive protein; and elevated erythrocyte sedimentation rate. Contrast-enhanced computed tomography identified aneurysms in branches of the pulmonary arteries (Figure 1). The final diagnosis was Hughes-Stovin syndrome.

Idiopathic and vascular diseases of the thorax have been the subject of recent publications in the radiology literature of Brazil[1–6]. Hughes-Stovin syndrome is a rare condition, characterized by the combination of multiple pulmonary artery aneurysms and peripheral venous thrombosis, that mainly affects males (80–90% of cases) between the second and fourth decades of life[7–11]. Although the lesions often affect arteries and veins simultaneously (in 68% of cases), isolated arterial or venous impairments are reported at frequencies of 25% and 7%, respectively[9,11].

In its typical presentation, Hughes-Stovin syndrome occurs in three stages[7–9,11]: in the first stage, there are signs and symptoms of thrombophlebitis; the second stage includes the formation and expansion of pulmonary artery aneurysms; and the third stage is characterized by aneurysmal rupture with massive hemoptysis, progressing to death. The formation of pulmonary aneurysms has been attributed to the weakening of the vessel walls by an inflammatory process. Other hypotheses proposed to explain these changes include septic embolism and angiodysplasia of the bronchial arteries[8,9,11]. Aneurysms can be single or multiple, unilateral or bilateral, and can even arise at other sites (in the iliac, femoral, popliteal, carotid, or hepatic arteries), although with a lower risk of rupture[9–11].

Some authors consider Hughes-Stovin syndrome an incomplete form of Behcet's disease, due to the similarity between the two in terms of the clinical, radiological, and pathological findings[7–11]. Therefore, Behcet's disease, which typically affects young males, is the main differential diagnosis[11]. The major (and mandatory) criterion for a diagnosis of Behcet's disease is oral ulcers that recur at least three times within 12 months, which should be